Pulsatility in ventricular assistance devices: A translational review focused on applied haemodynamics

Mickaël Lescroart, Jean-Louis Hébert, Flavien Vincent, Lee S. Nguyen

Pulsatility in ventricular assistance devices: A translational review focused on applied haemodynamics

Abbreviated title: Pulsatility in ventricular assistance devices

Mickaël Lescroart[a,*], Jean-Louis Hébert[a], Flavien Vincent[b], Lee S. Nguyen[c,d]

[a] *Institute of Cardiology, Pitié-Salpêtrière Hospital, AP-HP, Sorbonne University, 75013 Paris, France*

[b] *Cardiology Department of Interventional Cardiology for Coronary, Valves and Structural Heart Diseases, Institut Cœur Poumon; U1011, Inserm, Institut Pasteur de Lille, EGID, Université de Lille, 59000 Lille, France*

[c] *Department of Cardiac Surgery, Pitié-Salpêtrière Hospital, AP-HP, Sorbonne University, 75013 Paris, France*

[d] *Department of Research and Innovation (RICAP), CMC Ambroise Paré, 92200 Neuilly-sur-Seine, France*

* Corresponding author at: Service de Cardiologie, Institut de Cardiologie, CHU Pitié-Salpêtrière, 53 Boulevard de l'Hôpital, 75013 Paris, France.

E-mail address: lescroart.mickael@gmail.com (M. Lescroart).

Summary

Heart failure affects more than 30 million people worldwide and its prevalence is constantly rising. In 2020, heart transplantation is the only curative treatment, but left ventricular assistance devices (LVADs) are fully integrated into the decision algorithm for management of patients with advanced heart failure, with more than 20,000 devices implanted worldwide in the last decade. Intended to support cardiac output, LVADs remove the blood from the left ventricle and eject it into the proximal aorta. Whereas first-generation LVADs were pulsatile, second- and third-generation LVADs are more reliable, but create a laminar flow, with reduced (or absent) blood flow pulsatility. Concomitantly, several new adverse events, some of them lethal, appeared when continuous-flow LVADs started to be implanted, including acquired von Willebrand disease, gastrointestinal bleeding and aortic valve fusion or regurgitation. This review aims to apply models describing pulsatility (such as the Windkessel effect applied by Frank, Guyton's continuity model of venous return and Sunagawa's left ventricular-arterial coupling) to LVADs, to better understand the physiopathology in patients using continuous-flow devices. This review also covers the means of exploring pulsatility and adverse events associated with a reduction in pulsatility, as well as the possible ways for restoring pulsatility in patients implanted with an LVAD.

Résumé

L'insuffisance cardiaque touche plus de 30 millions de patients à travers le monde. Bien qu'à ce jour le seul traitement curatif de l'insuffisance cardiaque terminale reste la transplantation cardiaque, les LVAD sont pleinement intégrés dans l'algorithme de prise en charge, avec plus de 20 000 implantations au cours des 10 dernières années. Initialement pulsatiles, les LVAD de seconde et troisième générations sont à flux continu et ont permis d'améliorer la survie des patients, au prix d'une perte significative de la pulsatilité artérielle. Certains effets indésirables associés aux LVAD et engageant parfois le pronostic vital, ont été mis sur le compte de cette perte de pulsatilité, comme l'apparition d'une insuffisance aortique, d'un syndrome de Willebrand acquis ou d'une angiodysplasie digestive. Cette revue a pour objectif d'appliquer les concepts de l'hémodynamique classique et de la pulsatilité artérielle, développés par Frank, Guyton et Sunagawa, aux LVAD afin de mieux comprendre les complications associées à la perte de la pulsatilité. Cette revue traite également des effets

indésirables secondaires au flux laminaire, de leur prise en charge, et des différentes perspectives en développement pour restaurer artificiellement une pulsatilité sous LVAD.

KEYWORDS

LVAD;

Pulsatility;

Haemodynamics;

Adverse events;

Heart failure

Abbreviations: ADAMTS13, a disintegrin and metalloprotease with thrombospondin type I repeats 13; CF-LVAD, continuous-flow left ventricular assistance device; CF-VAD, continuous-flow ventricular assistance device; DO_2, oxygen delivery; Ea, end-systolic aortic elastance; Ees, end-systolic left ventricular elastance; HMW, high molecular weight; LVAD, left ventricular assistance device; PAoP, aortic pulse pressure; VAD, ventricular assistance device; VWF, von Willebrand factor.

Background

Human cardiac assistance started in 1953, as Gibbon successfully performed the first intraoperative cardiopulmonary bypass. The first implantation of a ventricular assistance device (VAD) in a human being was performed by Liotta in 1963, in rescue of a refractory cardiogenic shock during aortic valve replacement surgery; unfortunately, the patient died 4 days later. Heart transplantation, pioneered by Barnard in 1967, promoted the development of more refined VADs, which were initially conceived as pulsatile devices [1]. However, because of technological constraints, these VADs required the use of large pneumatic extracorporeal pumps, prone to malfunctions and failure, causing significant and often lethal complications. In the 1980s, experimental procedures demonstrated in bovines that continuous-flow devices were both efficient and safe [2]. These observations led to the emergence in the late 1990s of smaller intracorporeal pumps adapted to human patients. The feedback from patients assisted with long-term continuous-flow devices revealed deleterious associated side effects. The focus on underlying haematological disturbances, vascular shear stress and endothelial dysfunction induced by continuous flow on the one hand, and the application of basic science and haemodynamic concepts of pulsatility developed by 20th century scientists in a new “no or low” pulse physiology on the other hand, have both contributed to improve our understanding of left ventricular assistance device (LVAD) issues. The present paper aims to clarify the links between the loss of pulsatility and the incidence of such adverse events.

Definition of pulsatility and ventricular-arterial coupling: Basic principles

In clinical practice, arterial pulsatility may be explored by aortic pulse pressure (PAoP) measurement. PAoP, as measured in the aortic root, is defined as the difference between peak systolic pressure and end-diastolic pressure. PAoP depends on both ventricular stroke volume and aortic load. Thus, PAoP results from ventricular-arterial coupling. This concept may be explained by several models, described below.

In the 1950s, Guyton first hypothesized that cardiac output should remain equal to venous return (Fig. 1A and Fig. 1B) [3]. In his experiments carried out on freshly sacrificed dogs, neglecting cardiac pulsatility and the pulmonary vascular system, the right atrium was sutured to a continuous-flow pump throwing blood into the aortic root. In this way, Guyton highlighted that the resistive arteriolar system was 20-fold less compliant than the capacitive venous system. For him, cardiac output mainly

depended on the following factors: output of systemic venous return, mean right atrial pressure and mean circulatory pressure (i.e. the residual pressure within the circuitry at zero flow) [4].

In the 1990s, Sunagawa et al. developed the haemodynamic concept of ventricular-arterial coupling between the left ventricle and the arterial tree, each being represented as a chamber with its own elastic properties (Fig. 1D) [5]. Elastance is defined as the variation of pressure induced by a given variation of volume; the stiffer the system, the higher its volume elastance. The authors noticed that the left ventricular chamber and the arterial tree were characterized by their respective maximal end-systolic elastance (Ees for the left ventricle and Ea for the arterial tree). The intersection between the curves determines the amplitude of the stroke volume. The Ees/Ea ratio is called the ventricular-arterial coupling index [6]. It has been demonstrated that the efficiency of the coupling is optimal when Ea = Ees/2. In this model, a lower inotropism is represented by a lower Ees, and the adaptation will be left ventricular dilatation, thus optimizing cardiomyocyte contraction according to Starling's law (as a result of an immediate increased sensitivity of troponin C to calcium) and the Anrep effect (caused by a delayed increase of the intracellular calcium pool). The area of the pressure-volume curve represents the systolic external left ventricular myocardial work. An example in which Ees is elevated would be ventricular hypertrophy resulting from chronic hypertension, as the ventricular wall would abnormally stiffen. Although we still lack treatments that can lower solely Ees, the use of renin-angiotensin-aldosterone system inhibitors may reduce the slope of Ea, thus lowering left ventricular afterload, reducing left ventricular external stroke work and enhancing left ventricular stroke volume and, finally, cardiac output too.

Ultimately, the vascular system cannot be defined only as a resistive system. Two properties deserve attention: the Windkessel effect and pulse wave reflection. First used by German firemen to extinguish fires, the Windkessel effect converts a pulsatile flow generated by a water hand pump into a continuous flow. This model partly accounts for the property of the aortic tree to give back during diastole the pressure energy accumulated in its walls during the previous ventricular ejection phase, thus partly damping the pulse pressure generated at the aortic root by the previous ventricular ejection. A three-element Windkessel model is commonly used to determine arterial system characteristics, i.e. resistance (R), compliance (C), and characteristic impedance of the circuitry (Zc). In a simplified two-element model, as initially described by Otto Frank, the RC time constant predicts diastolic aortic pressure as $P_{dia}(t) = P_{es}e^{-t/RC}$ [7], with P_{es} being end-systolic pressure, and RC being

the time constant (Tau) of the system.

Several studies have shown the link between the amplitude of aortic pulse pressure and cardiovascular morbidity and mortality [8]. Cardiac systolic contraction transmits energy to the stroke volume, but also to the arteries in the form of a pressure wave progressing forward through the arterial tree, and then reflecting backwards on the aortic bifurcations to the proximal aorta (Fig. 1C). In younger patients with high systemic arterial compliance, the reflected wave is dampened; it progresses with low velocity (4 m/s) and surges after aortic valve closure, leading to a dicrotic notch, easily identified following the catacrotic notch on the aortic pressure recorded at the level of the aortic root. Conversely, the pressure wave is faster in elderly patients (up to 10 m/s) because of the high stiffness of the arterial system. Then, the reflection wave (of the previous heartbeat) happens earlier, during the terminal ejection period, before aortic valve closure, thus enhancing both aortic end-systolic and pulse pressures. As a result, left ventricular afterload and left ventricular work are both increased to ensure a steady cardiac output. Moreover, heart rate decreases linearly with age, thus lowering cardiac index both at rest and at stress. Considering the physiological concepts described previously, we can postulate that a continuous flow in a VAD might significantly reduce the backward reflection wave as generated by the physiological pulsatile flow and would therefore improve the anterograde flow of the pump.

Another relevant approach to pulsatility focuses on energy flow. To approach energy flow, formulae have been proposed, such as energy equivalent pressure expressed in mmHg, which measures haemodynamic energy per unit of pumped volume, and surplus haemodynamic energy expressed in ergs/cm^3. EEP and SHE formulae could be written as: energy equivalent pressure (mmHg) = (∫Q.Pdt)/(∫Qdt), where Q is flow, P is pressure and dt is time first derivative; and surplus haemodynamic energy (mmHg) = (energy equivalent pressure – mean arterial pressure). Undar et al. noted the inadequacy of simply stating the pulse pressure, and suggested that using an energy gradient would make more sense than just using a pressure gradient [9]. Shepard et al. assumed that additional energy delivered on account of pulsatile flow would help to keep the microcirculation open [10]. Mathematical modelling has reported that a pulsatile flow provides 2.4 times as much energy as a non-pulsatile flow [11]. These energy variables, however, remain quite theoretical and therefore have not been studied extensively in circulatory support devices.

LVADs in 2020

In France in 2020, two types of CF-LVADs are commonly implanted, i.e. axial and centrifugal (Fig. 2). Jarvik 2000® (Jarvik Heart, Inc., New York, NY, USA) and HeartMate II™ (Thoratec Corporation, Pleasanton, CA, USA) are axial devices in which an Archimedes' screw provides blood suction from the left ventricle to the aorta, whereas HeartWare™ (Medtronic, Dublin, Ireland) and HeartMate III™ (Thoratec Corporation, Pleasanton, CA, USA) are centrifugal devices, equipped with a fully electromagnetic spinning pump. LVADs can be implanted as a bridge to transplant (26%), a bridge to candidacy (23%), when a temporary contraindication to register a patient on cardiac transplant list is obvious, or as a destination therapy (51%) when no healing of the patient is expected [12]. Precise evaluation of right ventricular function before implantation is necessary, as right ventricular failure occurs in up to 40% of cases after LVAD implantation. However, assessment of right ventricular function is challenging [13]. Transthoracic echocardiography is the first-line tool for characterizing right ventricular morphology and systolic function, and for detecting tricuspid regurgitation to better assess right heart failure after LVAD implantation [14]. Interestingly, tricuspid annular plane systolic excursion (TAPSE) measurement does not improve right heart failure prediction, whereas right ventricular speckle tracking significantly does. A right ventricular/left ventricular end-diastolic diameter > 0.7 is associated with an odds ratio of 11 (95% confidence interval 3.0–43.6; $P = 0.001$) for right heart failure after LVAD implantation [15]. Nevertheless, right ventricular assessment remains one of the most challenging concerns before LVAD implantation, and readers can refer to Bellavia et al. for more details [14]. After implantation, LVAD requires anticoagulation with vitamin K antagonists (targeting an international normalized ratio of 2–3) and antiplatelet therapy, usually with aspirin 75 mg/day. A monitor provides information about pump power, pump outflow (calculated from pump power, pump speed and haematocrit) and about the remaining charge level of the battery. At the bedside, the pump rotation speed is the device's only flexible variable. According to guidelines, speed rotation must be guided by aortic valve opening, assessed by echocardiography. LVAD support should aim to open the aortic valve every two or three beats, unless it would result in overloading or underloading the left ventricle [16]. It is important to keep in mind that the reduction of the rotary pump's speed will decrease both the mean arterial pressure and the wash out of the pump, leading to an increased risk of pump thrombosis. LVAD thrombosis occurs in 2–13% of patients with a continuous-flow LVAD (CF-LVAD) (axial flow: 4–13%; centrifugal flow: 8%) [17]. The MOMENTUM III study reported no event in

patients implanted with the HeartMate III™ versus a 10.4% rate of events in patients implanted with the HeartMate II™ [18]. Current LVADs are continuous-flow devices, but artificial pulsatility can be restored by modulation of the speed rotation algorithm.

From basic science concepts to clinical implications

Invasive catheterization provides the key to understanding haemodynamic changes with an LVAD (Fig. 3). In a recent study of patients implanted with a CF-LVAD [19], the authors focused on the haemodynamic effects of a ramp (a progressive increase in the LVAD rotation speed) by analysing right- and left-sided pressures using simultaneous high-fidelity recordings.

In normal subjects at rest and in the supine position, pulmonary wedge pressure is around 10 mmHg and should not be > 12 mmHg. Usually, it remains higher than mean right atrial pressure, which stays at around 3 mmHg. When the pump speed rises from 9000 to 10,000 RPM, pulmonary wedge pressure falls below the right atrial pressure level because the pump exerts a suction effect on the pulmonary blood venous return through the left ventricle; this may shorten the transit time of red blood cells through the pulmonary capillaries, and lead to decreased haemoglobin oxygenation. Indeed, the normal mean pulmonary capillary transit time of around 0.75 seconds in recumbent adults at rest is sufficient through healthy lungs to ensure normoxaemia, but if alveolar diffusion is decreased, accelerated pulmonary capillary transit may lead to systemic hypoxaemia.

As systemic arterial pressure is preserved as a result of LVAD anterograde flow, the heart rate remains unchanged whatever the pump rotation rate, because the baroreflex loop is not stimulated, whereas mean right atrial pressure remains in the normal range, because venous return is also maintained.

Instead of a centrifugal pump sutured in series between the vena cava and the aorta, as in Guyton's model, circulation in an LVAD may be modelled as a double-parallel pumping system, with the left ventricle ejecting through the aortic valve on the one hand, and the LVAD through its own extra cardiac circuitry up to the ascending aorta on the other hand. This device enables us to validate in humans *in vivo* Guyton's observation that increasing cardiac flow induces higher aortic pressures and lower pulmonary wedge pressure and pulmonary artery pressure, whereas systemic venous return and right atrial pressure remain stable because of the preserved anterograde driving pressure through the systemic circulation.

The transaortic pressure gradient between lowered peak ventricular pressure and synchronous aortic pressure widens as the pump speed increases, resulting in chronic closing of the aortic valve, as the aortic pressure is constantly higher than the concomitant ventricular pressure. Low left ventricular pressure has two causes: end-stage heart failure with reduced left ventricular stroke index, and the fraction of this volume that is diverted by the LVAD to be reinjected into the aortic root; together with possible residual stroke volume in cardiac cycles in which peak ventricular pressure is high enough to intermittently open the aortic cusps. This represents the exact opposite condition to that of aortic stenosis or obstructive cardiomyopathy, in which left ventricular pressure constantly overruns aortic pressure. Otherwise, a pulse pressure pattern is artificially induced at the aortic root by pump speed modulation, as left ventricular pressure remains lower than aortic pressure. As a result, the aortic valve is constantly closed, with a high risk of valvular thrombosis or sclerosis. If we focus on both the aortic and left ventricular pressure curves in Fig. 3, we notice that peak aortic pressure peak constantly occurs after peak left ventricular pressure. This is probably caused, in part, by the delay induced by the longer extracardiac circuitry between the LVAD pump and the aortic root compared with the short path crossed by the stroke volume through the aortic valve when it opens. Thus, the gradient between peak aortic pressure and synchronous ventricular pressure decay, observed at each loading level of the left ventricle, is constantly clearly larger (up to 60 mmHg) than the 20–40 mmHg transaortic pressure gradient. We identified this true gradient in Fig. 3 as the effective gradient. Moreover, this gradient occurs during the phase of active ventricular relaxation that produces a supplementary suction effect on the aortic cusps, favouring even more valvular eversion and chronic aortic regurgitation. The shorter the circuitry of the device, the earlier the peak aortic pressure and the lower the effective gradient should be, and hence the risk of developing aortic regurgitation.

Aortic regurgitation in patients with an LVAD creates a partial retrograde recirculation which reduces the effective anterograde aortic flow through the LVAD circuitry. Quantifying the degree of recirculation remains a diagnostic challenge [20]. Chronic valve exposure to aortic regurgitation may lead to aortic valve thrombosis and commissural fusion. Jorde et al. showed that one third of patients with an LVAD will develop moderate-to-severe aortic regurgitation after 3 years, needing surgical aortic replacement or heart transplant. If surgical replacement is needed, bioprostheses are preferred over mechanical valves, because of the lower risk of aortic root thrombosis [21]. The use of endovascular rapid-deployment valves is subject to caution, as only a few cases have been reported

so far, whereas issues have been described regarding the incidence of valve thrombosis with sutureless bioprosthetic valves [22].

Hence, these multiple synchronous high-fidelity pressure recordings offer insight into the physiopathology of the main risks of aortic valve sclerosis, thrombosis and eversion, leading to chronic aortic regurgitation.

Adverse events associated with CF-LVADs

Numerous adverse events are associated with long-term implantation of the current generation of LVADs, but not all are related to the lack of pulsatility (Central illustration).

Haematological consequences

LVAD-induced haemolysis, defined as serum free haemoglobin > 40 mg/dL or lactate dehydrogenase > 600 IU/L [23], increased sharply with the development of continuous-flow devices. Although this issue is not a consequence of lack of pulsatility, but rather a result of the device's mechanical characteristics, it still deserves attention. First, haemolysis requires red blood cell transfusion, with the risk of alloimmunization in patients on the transplant waiting list. Next, Bartoli et al. demonstrated in 2018 that plasma free haemoglobin released during haemolysis is bound to "a disintegrin and metalloprotease with thrombospondin type I repeats 13" (ADAMTS13), and activates von Willebrand factor (VWF), which can initiate clot formation in the pump, leading to a prothrombotic state [24]. In this 30-patient study, nine patients who developed LVAD thrombosis previously experienced more haemolytic events. Picod et al. recently highlighted that cardiac output may be the main determinant of oxygen delivery (DO_2) during haemolysis [25]. Hence, patients at highest risk are those who are unable to increase their cardiac output to maintain their DO_2 above the hypoxia threshold. This is obviously the case for patients with an LVAD, in whom tissue hypoxia should be systematically sought. Furthermore, recent studies suggest that for to prevent haemolysis caused by the small diameter of the HeartMate II™ device, the impeller must spin up to 8000–12,000 RPM, leading to important shear stress on red blood cells. Third-generation devices (HeartWare™ and HeartMate III™) create a fully levitated electromagnetic centrifugal flow with a larger pump diameter, thus allowing lower rotational speeds (2000–3000 RPM), and significantly reducing haemolysis issues. Nonetheless, the involvement of oxygen extraction and DO_2 may need further investigation.

The transition from first-generation pulsatile-flow VADs to second-generation continuous-flow VADs (CF-VADs) was associated with longer survival, but with a tremendous increase in gastrointestinal and cutaneous-mucosal bleeding complications too. Almost 50% of patients still experienced bleeding 2 years after implantation of the latest generation of VADs [26]. The functional abnormalities of VWF are considered one of the main risk factors for bleeding with a CF-VAD.

A focus on basic science may provide better understanding in this domain. VWF is a multimeric glycoprotein, synthesized in both platelets and endothelial cells, and stored in Weibel-Palade bodies. This protein supports different aspects of the haemostatic process, interacting with platelets, collagen and factor VIII [27]. Fundamental studies of the structure-function relationships of VWF demonstrated that the regulation of this protein is unique, in that VWF can change its steric conformation in response to shear stress. VWF circulates in the bloodstream as a globular protein, and exposure to increased shear forces drives the protein into an elongated conformation [28]. This change unmasks the A2 cleavage domain site to interact with ADAMTS13 protease, promoting its proteolysis and the loss of the highest molecular weight multimers of VWF. As the largest multimers are the most potent in terms of interaction with platelets and collagen, the lack of high molecular weight (HMW) multimers exposes patients to bleeding diathesis. Thus, patients with a congenital HMW multimer defect (von Willebrand disease type 2A) present bleeding events mainly from cutaneous and mucosal origins, such as gastrointestinal angiodysplasia.

The VWF HMW multimer defect (i.e. acquired von Willebrand syndrome type 2A) is almost constant with a CF-VAD [29], regardless of the type of design (axial or centrifugal) [30]. Previous in vitro studies in a mock circulatory loop in the absence of endothelium demonstrated that the supraphysiological shear stress induced by the CF-VAD leads to the degradation of HMW multimers within a few minutes via a mechanical-enzymatic process [31].

The reduction in pulsatility with a CF-VAD could also be involved in the HMW multimer defect. The extent of the reduction in arterial pulsatility depends on the balance between the device flow rate and the residual native left ventricular pulsatility. Wever-Pinzon et al. observed that bleeding risk was correlated with residual pulsatility, with a 4-fold increase in risk of non-surgical bleeding in HeartMate II© recipients with a low pulsatility index compared with patients with a high pulsatility index [32].

Similarly, in aortic stenosis, one can observe both a high shear stress pathological condition and a reduction in pulsatility, leading in some cases to an acquired VWF syndrome type 2A, which can be

implicated in the development of Heyde's syndrome [33]. Several studies observed a rapid (within minutes) and complete normalization of the VWF multimer profile after valve replacement (mainly transaortic valve replacement procedures). This recovery was concomitant with the release of both VWF propeptide and VWF antigen, strongly suggesting that an endothelial release of new VWF occurs as soon as the blood flow returns to physiological pulsatile conditions [31].

The relationship between VWF and residual pulsatility was recently further studied in an animal model [34]. This work revealed that the magnitude of HMW multimer degradation was modulated by pulsatility level in the high-shear stress condition of a CF-VAD. In addition, the authors observed that restoring pulsatility triggered an acute endothelial release of VWF antigen and other molecules contained in Weibel-Palade bodies, such as angiopoietin-2. These findings were strongly suggestive of an acute release of new VWF multimers from the endothelial cells in response to the increase in arterial pulsatility. Moreover, they reported a similar observation in a patient undergoing sequential changes in pulsatility after implantation of an extracorporeal membrane oxygenator followed by a pulsatile-flow VAD (Carmat total artificial heart; Carmat SA, Vélizy-Villacoublay, France).

Overall, preservation of pulsatility during continuous-flow mechanical circulatory support could mitigate the acquired VWF defect associated with VADs, and new continuous-flow devices with pulsatile properties might be an option for reducing the bleeding burden of patients (Fig. 4).

Finally, platelet dysfunction commonly occurs in patients with LVADs. In vitro studies have reported more reduced platelet activation and aggregation with continuous flow than with pulsatile flow [35]. Steinlechner et al. conducted a study in 24 patients with LVADs with significant platelet dysfunction, not always attributable to acquired von Willebrand syndrome [36]. Indeed, platelet dysfunction was described in chronic heart failure even before LVAD implantation. In a mock loop model, a pulsatile system significantly increased nitric oxide synthase production in red blood cells. As nitric oxide increased erythrocyte compliance by nitrosylation of its cytoskeletal proteins, pulsatile flow enhanced microcirculation. Finally, the mean arterial pressure required for normal capillary perfusion is increased under continuous flow compared with pulsatile flow, meaning that patients with continuous-flow devices are more prone to capillary collapse.

Cerebral outcomes

The INTERMACS registry reported that 6 months after LVAD implantation, stroke remained the major cause of death, for up to 4 years [12]. From 2012 to 2015, up to 10% of patients with a CF-LVAD had at least one stroke event, with an incidence rate of 0.123 strokes per patient-year. Of these, 51% were ischaemic strokes, whereas 48% were of haemorrhagic origin. Haemorrhagic strokes had a worse prognosis, as 30-day survival was 45% compared with 80% in case of ischaemic strokes.

The association between pulsatility and stroke remains elusive. Whereas there is a strong association between stroke occurrence and abnormally increased pulsatility, lack of pulsatility has not been clearly established as a risk factor for such cardiovascular events [37, 38].

The MOMENTUM 3 study suggested that restoring pulsatility in LVADs should decrease ischaemic strokes. Nonetheless, cerebral events are often the result of device-associated adverse events, such as pump thrombosis, gastrointestinal bleedings, etc., and are not necessarily linked to a lack of pulsatility [26]. It was demonstrated in the MOMENTUM 3 study that reduced stroke rate was linked to better washout of the pump, but not to restored vascular physiology.

However, several physiological findings may provide some insight into the pathology. Although arteriolar flow is known to be laminar and continuous, Rappaport et al. observed that a low pulsatile flow pattern still remained in the capillary beds [39]. This would lead to a slowing of cerebral transit time in the diastolic phase, and facilitate gas exchange through the watertight brain capillary endothelium [40]. In CF-LVADs, increased diastolic blood velocity could impair oxygen kinetics. Nonetheless, current studies rather suggest that cerebral oxygenation is preserved in CF-LVADs [41]. Grubhofer et al. measured physiological cerebral oxygenation by means of near infrared spectroscopy [42], whereas Hoshi et al. showed that cytochrome oxidase aa3 (a marker of cellular hypoxia) was identical in both pulsatile-flow and continuous-flow circulations, suggesting that oxygen delivery is appropriate with CF-LVADs [43].

Cerebral homeostasis aims to keep cerebral artery blood flow constant under any cerebral perfusion pressure level. CF-LVADs constitute a high flow-low resistance model, although cerebral autoregulation may be preserved. Indeed, Cornwell et al. showed that, during a sit-to-stand manoeuvre, mean cerebral artery velocity was identical in patients with a CF-LVAD and healthy controls [44].

Finally, a low-pulsatility system induces endothelial dysfunction, with decreased nitric oxide production in CF-LVADs compared with pulsatile devices. Although cerebrovascular physiology seems

to be preserved in continuous-flow systems, Yoshioka et al. recently showed induced arteriolar fragility and microangiopathy pattern inducing brain cortical microbleedings in this context [45].

Gastrointestinal bleeding

Although the MOMENTUM 3 study reported a significant reduction in pump thrombosis, no improvement has been reported concerning gastrointestinal bleeding. Bleeding remains the most common adverse event: around 60% of patients with an LVAD experienced gastrointestinal bleeding. The mean time to a bleeding event was 88 days. Arteriovenous malformation and angiodysplasia mostly explained this issue. Analogy was made with angiodysplasia development in Heyde's syndrome, first described in 1958.

As mentioned previously, gastrointestinal bleeding is linked to acquired von Willebrand syndrome. The haemostatic effect of VWFs is proportional to their size: the smallest are those with the least activity. As the shear stress of the pump increases, proteolysis of HMW multimers designed to protect VWF from cleaving occurs, VWFs shorten and the lack of pulsatility leads to endothelial dysfunction and reduced production of VWF. Furthermore, VWF synthesis leads to the constitution of Weibel-Palade bodies, which stock angiopoietin-2. VWF is therefore involved in both haemostasis and angiogenesis [46].

In a 2010 retrospective study, Crow et al. described a 10-fold increase in gastrointestinal bleeding with non-pulsatile devices (63 events/100 patient-years versus 6.8/100 patient-years with pulsatile devices), without any significant impact on mortality [47]. Nonetheless, haemorrhagic events were closely linked to thrombotic burden, and preventing gastrointestinal bleeding could prevent cerebral stroke and blood transfusion. Continuous-flow exposure led to gastrointestinal arteriovenous shunt openings, resulting from the lack of sympathetic stress, and to the loss of microcirculation vasoregulation. The work by Demirozu et al. on gastrointestinal bleeding with HeartMate II™ revealed that arteriovenous malformations might develop all along the digestive tract [48].

Current guidelines advise gastrointestinal endoscopy for diagnostic strategy, and therapeutic management is mainly based on modulation of both anticoagulation and antiplatelet therapy [49]. Nonetheless, the TRACE study concluded that reduced treatment in response to bleedings did not lead to lower haemorrhagic events, but enhanced thrombotic burden [50]. When conventional endoscopy fails to identify the source of bleedings, capsule endoscopy, computed tomography scan

and angiography may be used, with a diagnostic yield of 40%. Treatment is based on endoscopy and surgery, lowering of pump speed and transfusion of VWF/factor VIII concentrates. Digestive vasoactive drugs, such as octreotide (a somatostatin analogue), have been used for treatment and secondary prevention, with mild efficacy reported in the literature.

In the 1990s, a highly specific concentrate of VWF (Wilfactin®; LFB, Les Ulis, France) was developed to cure patients who were resistant to desmopressin. First developed for constitutive von Willebrand syndrome, Wilfactin® was recently used to treat gastrointestinal bleedings in patients with an LVAD, after failure of conventional treatment strategies [51]. A phase 3 randomized multicentre study (the PHAM study), ongoing since 2015, aims to demonstrate a reduction in bleeding occurrence in patients receiving prophylactic treatment with Wilfactin® after implantation of continuous-flow mechanical support. Included patients need to present a functional defect in VWF measured between day 2 and day 4 after LVAD implantation. So far, gastrointestinal bleeding is one of the major burdens of LVADs, and fully highlights the consequences of a lack of pulsatility.

Restoring a pulse

To prevent the deleterious effects of continuous flow, engineers and physicians are challenged to restore some pulse pressure. Current guidelines advise maintaining mean arterial pressure < 80 mmHg in CF-LVADs, as hypertension is the main risk factor for stroke with LVADs. The pulse pressure threshold must be suitable for even intermittent aortic valve opening assessed by transthoracic echocardiography. To what extend the pressure needs to be pulsed remains an unanswered question [49].

Jarvik 2000® was the first CF-LVAD to use a speed variation algorithm that delivered a lowering of the pump speed for 8 seconds each minute. HeartWare™ introduced similar algorithms, named Lavare or Q-pulsed cycles, which allowed the aortic valve to open, and resulted in a better washout of the aortic root, with the aim of preventing clot formation. Nonetheless, pump speed modulation of this device occurred only every 30 or 60 seconds. For restoring a more suitable condition, HeartMate III™ recently developed the "artificial pulse", the most “physiological” algorithm to date in terms of beats per minute, by varying the speed of the pump every 2 seconds. However, the HeartMate III™ models tested currently can only generate a PAoP of about 10–20 mmHg [52]. By their nature, current technologies, based on turbines rotating at very high speeds with high inertia, have limited ability to

restore any “physiological” pulsatility. It is indeed difficult to vary the speed of rotation of the turbine, whereas power consumption is increased by up to about 20–40% with these algorithms of modulation in all pulsatile modes, compared with constant speed modes [53].

Another question that has arisen concerns synchronization of pulsatility. There are three basic approaches to synchronization timing: copulsation, counterpulsation and asynchronous mode. Counterpulsation achieves a maximum unloading of the left ventricle as determined by stroke work and myocardial wall stress [54]. Copulsation maximizes haemodynamic conditions in the aorta by producing greater pulse pressure and pulse energy [55]. Asynchronous mode probably provides these two basic benefits in an alternating fashion, as the phase shift moves from copulsation to counterpulsation. If the aim of restoring pulsatility is left ventricular recovery, then it is speculated that counterpulsation is optimal as first choice, while reduction of adverse events related to a lack of pulsatility may be better achieved by a copulsation mode. The 2015 paper by Ising et al. documented different synchronization techniques with the HeartWare™ device, both in mock loops and some animal trials [56]. The asynchronous mode in animals resulted in a pulse pressure of < 40 mmHg in amplitude, and pressure change rate was quite low in all modes. Copulsation generated the largest peak VAD flows and the greatest amplitude difference in flows. This could be important in terms of endothelial shear stress, which is a determinant in the various processes mentioned above. Pirbodaghi et al. focused on left ventricular work, and cautioned against the fact that copulsation resulted in backflow through the pump during diastole and increased the workload of the heart [54]. The data of Soucy showed that copulsation unloaded the left ventricle to a much lesser extent than counterpulsation [44]. It remains difficult to draw a firm conclusion from these results, and there have not been enough studies to date allowing a comparison between techniques. Further investigations are still needed.

Conclusions

Advanced heart failure is commonly associated with low pulsed pressure as systolic function decreases. Restoring pulsatility is part of the therapeutic field, and the American guidelines for ischaemic heart failure management encourage external counterpulsation to improve clinical outcomes [57]. Similarly, restoring pulsatility in patients with an LVAD may improve functional

outcomes and survival. Current-generation LVADs cannot attain adequate physiological pulsatility and overcoming this problem may well be the next technological challenge in the field.

Acknowledgments

We thank our colleagues at the Institute of Cardiology of Pitié-Salpêtrière University Hospital and the Institute of Cardiometabolism And Nutrition (ICAN) for contributing to this manuscript. Specific acknowledgments must be addressed to Didier Payen, Pierre Squara, Sophie Susen and Alexandra Schmidt for their key contributions. Finally, we thank Atta Behfar and Philippe Morimont for giving their consent to reproduce figures from their publications.

Sources of funding

None.

Disclosure of interest

L. S. N. Research grants from the **Fédération Française de Cardiologie** and the **Société Française de Cardiologie**. Consulting fees from the company **CorWave** in 2016.

F. V. Research grant from the **Fédération Française de Cardiologie**.

The other authors declare that they have no conflicts of interest concerning this article.

References

[1] Flecher E, Joudinaud T, Grinda JM. [Mechanical cardiac assistance and artificial heart: historical perspectives]. Ann Chir 2006;131:473-8.

[2] Yada I, Golding LR, Harasaki H, et al. Physiopathological studies of nonpulsatile blood flow in chronic models. Trans Am Soc Artif Intern Organs 1983;29:520-5.

[3] Guyton AC. Determination of cardiac output by equating venous return curves with cardiac response curves. Physiol Rev 1955;35:123-9.

[4] Beard DA, Feigl EO. Understanding Guyton's venous return curves. Am J Physiol Heart Circ Physiol 2011;301:H629-33.

[5] Sunagawa K, Sagawa K, Maughan WL. Ventricular interaction with the loading system. Ann Biomed Eng 1984;12:163-89.

[6] Morimont P, Lambermont B, Ghuysen A, Gerard P, Kolh P, D'Orio V. [Ventriculo-arterial coupling: from concepts to clinical applications]. Réanimation 2009;18:201-6.

[7] Westerhof N, Lankhaar JW, Westerhof BE. The arterial Windkessel. Med Biol Eng Comput 2009;47:131-41.

[8] Mitchell GF, Hwang SJ, Vasan RS, et al. Arterial stiffness and cardiovascular events: the Framingham Heart Study. Circulation 2010;121:505-11.

[9] Undar A. Myths and truths of pulsatile and nonpulsatile perfusion during acute and chronic cardiac support. Artif Organs 2004;28:439-43.

[10] Shepard RB, Simpson DC, Sharp JF. Energy equivalent pressure. Arch Surg 1966;93:730-40.

[11] Baric D. Why pulsatility still matters: a review of current knowledge. Croat Med J 2014;55:609-20.

[12] Kirklin JK, Pagani FD, Kormos RL, et al. Eighth annual INTERMACS report: Special focus on framing the impact of adverse events. J Heart Lung Transplant 2017;36:1080-6.

[13] Sanz J, Sanchez-Quintana D, Bossone E, Bogaard HJ, Naeije R. Anatomy, Function, and Dysfunction of the Right Ventricle: JACC State-of-the-Art Review. J Am Coll Cardiol 2019;73:1463-82.

[14] Bellavia D, Iacovoni A, Scardulla C, et al. Prediction of right ventricular failure after ventricular assist device implant: systematic review and meta-analysis of observational studies. Eur J Heart Fail 2017;19:926-46.

[15] Neyer J, Arsanjani R, Moriguchi J, Siegel R, Kobashigawa J. Echocardiographic parameters associated with right ventricular failure after left ventricular assist device: A review. J Heart Lung Transplant 2016;35:283-93.

[16] Bouchez S, Van Belleghem Y, De Somer F, De Pauw M, Stroobandt R, Wouters P. Haemodynamic management of patients with left ventricular assist devices using echocardiography: the essentials. Eur Heart J Cardiovasc Imaging 2019;20:373-82.

[17] Dang G, Epperla N, Muppidi V, et al. Medical Management of Pump-Related Thrombosis in Patients with Continuous-Flow Left Ventricular Assist Devices: A Systematic Review and Meta-Analysis. ASAIO J 2017;63:373-85.

[18] Mehra MR, Uriel N, Naka Y, et al. A Fully Magnetically Levitated Left Ventricular Assist Device - Final Report. N Engl J Med 2019;380:1618-27.

[19] Rosenbaum AN, Frantz RP, Kushwaha SS, Stulak JM, Maltais S, Behfar A. Novel Left Heart Catheterization Ramp Protocol to Guide Hemodynamic Optimization in Patients Supported With Left Ventricular Assist Device Therapy. J Am Heart Assoc 2019;8:e010232.

[20] Akiyama D, Nishimura T, Sumikura H, et al. Accurate Method of Quantification of Aortic Insufficiency During Left Ventricular Assist Device Support by Thermodilution Analysis: Proof of Concept and Validation by a Mock Circulatory System. Artif Organs 2018;42:954-60.

[21] Jorde UP, Uriel N, Nahumi N, et al. Prevalence, significance, and management of aortic insufficiency in continuous flow left ventricular assist device recipients. Circ Heart Fail 2014;7:310-9.

[22] Yanagawa B, Verma S, Mazer CD. Subclinical Valve Thrombosis in Sutureless Bioprosthetic Valves. J Am Heart Assoc 2017;6.

[23] Cowger JA, Romano MA, Shah P, et al. Hemolysis: a harbinger of adverse outcome after left ventricular assist device implant. J Heart Lung Transplant 2014;33:35-43.

[24] Bartoli CR, Zhang D, Kang J, et al. Clinical and In Vitro Evidence That Subclinical Hemolysis Contributes to LVAD Thrombosis. Ann Thorac Surg 2018;105:807-14.

[25] Picod A, Blanchard F, Cohen Y. Cardiac output drives tolerance of acute hemolysis. Intensive Care Med 2018;44:1362-3.

[26] Mehra MR, Naka Y, Uriel N, et al. A Fully Magnetically Levitated Circulatory Pump for Advanced Heart Failure. N Engl J Med 2017;376:440-50.

[27] Rauch A, Caron C, Susen S, Goudemand J. [Von Willebrand factor and von Willebrand disease: novel insights]. Rev Francoph Lab 2014;2014:53-63.

[28] Siedlecki CA, Lestini BJ, Kottke-Marchant KK, Eppell SJ, Wilson DL, Marchant RE. Shear-dependent changes in the three-dimensional structure of human von Willebrand factor. Blood 1996;88:2939-50.

[29] Uriel N, Pak SW, Jorde UP, et al. Acquired von Willebrand syndrome after continuous-flow mechanical device support contributes to a high prevalence of bleeding during long-term support and at the time of transplantation. J Am Coll Cardiol 2010;56:1207-13.

[30] Susen S, Rauch A, Van Belle E, Vincentelli A, Lenting PJ. Circulatory support devices: fundamental aspects and clinical management of bleeding and thrombosis. J Thromb Haemost 2015;13:1757-67.

[31] Van Belle E, Rauch A, Vincentelli A, et al. Von Willebrand factor as a biological sensor of blood flow to monitor percutaneous aortic valve interventions. Circ Res 2015;116:1193-201.

[32] Wever-Pinzon O, Selzman CH, Drakos SG, et al. Pulsatility and the risk of nonsurgical bleeding in patients supported with the continuous-flow left ventricular assist device HeartMate II. Circ Heart Fail 2013;6:517-26.

[33] Vincent F, Rauch A, Loobuyck V, et al. von Willebrand Factor for Aortic Valve Intervention: From Bench to Real-Time Bedside Assessment. Circ Res 2018;122:1499-500.

[34] Vincent F, Rauch A, Loobuyck V, et al. Arterial Pulsatility and Circulating von Willebrand Factor in Patients on Mechanical Circulatory Support. J Am Coll Cardiol 2018;71:2106-18.

[35] Zhao XM, Wu YP, Cai HX, et al. The influence of the pulsatility of the blood flow on the extent of platelet adhesion. Thromb Res 2008;121:821-5.

[36] Steinlechner B, Dworschak M, Birkenberg B, et al. Platelet dysfunction in outpatients with left ventricular assist devices. Ann Thorac Surg 2009;87:131-7.

[37] Chuang SY, Cheng HM, Bai CH, Yeh WT, Chen JR, Pan WH. Blood Pressure, Carotid Flow Pulsatility, and the Risk of Stroke: A Community-Based Study. Stroke 2016;47:2262-8.

[38] Harris S, Reyhan T, Ramli Y, Prihartono J, Kurniawan M. Middle Cerebral Artery Pulsatility Index as Predictor of Cognitive Impairment in Hypertensive Patients. Front Neurol 2018;9:538.

[39] Rappaport MB, Bloch EH, Irwin JW. A manometer for measuring dynamic pressures in the microvascular system. J Appl Physiol 1959;14:651-4.

[40] Wardlaw JM, Dennis MS, Merrick MV, Warlow CP. Relationship between absolute mean cerebral transit time and absolute mean flow velocity on transcranial Doppler ultrasound after ischemic stroke. J Neuroimaging 2002;12:104-11.

[41] Stohr EJ, McDonnell BJ, Colombo PC, Willey JZ. CrossTalk proposal: Blood flow pulsatility in left ventricular assist device patients is essential to maintain normal brain physiology. J Physiol 2019;597:353-6.

[42] Grubhofer G, Mares P, Rajek A, et al. Pulsatility does not change cerebral oxygenation during cardiopulmonary bypass. Acta Anaesthesiol Scand 2000;44:586-91.

[43] Hoshi Y, Hazeki O, Tamura M. Oxygen dependence of redox state of copper in cytochrome oxidase in vitro. J Appl Physiol (1985) 1993;74:1622-7.

[44] Cornwell WK, 3rd, Tarumi T, Aengevaeren VL, et al. Effect of pulsatile and nonpulsatile flow on cerebral perfusion in patients with left ventricular assist devices. J Heart Lung Transplant 2014;33:1295-303.

[45] Yoshioka D, Okazaki S, Toda K, et al. Prevalence of Cerebral Microbleeds in Patients With Continuous-Flow Left Ventricular Assist Devices. J Am Heart Assoc 2017;6:e005955.

[46] Kataria R, Jorde UP. Gastrointestinal Bleeding During Continuous-Flow Left Ventricular Assist Device Support: State of the Field. Cardiol Rev 2019;27:8-13.

[47] Crow S, John R, Boyle A, et al. Gastrointestinal bleeding rates in recipients of nonpulsatile and pulsatile left ventricular assist devices. J Thorac Cardiovasc Surg 2009;137:208-15.

[48] Demirozu ZT, Radovancevic R, Hochman LF, et al. Arteriovenous malformation and gastrointestinal bleeding in patients with the HeartMate II left ventricular assist device. J Heart Lung Transplant 2011;30:849-53.

[49] Feldman D, Pamboukian SV, Teuteberg JJ, et al. The 2013 International Society for Heart and Lung Transplantation Guidelines for mechanical circulatory support: executive summary. J Heart Lung Transplant 2013;32:157-87.

[50] Katz JN, Adamson RM, John R, et al. Safety of reduced anti-thrombotic strategies in HeartMate II patients: A one-year analysis of the US-TRACE Study. J Heart Lung Transplant 2015;34:1542-8.

[51] Fischer Q, Huisse MG, Voiriot G, et al. Von Willebrand factor, a versatile player in gastrointestinal bleeding in left ventricular assist device recipients? Transfusion 2015;55:51-4.

[52] Netuka I, Sood P, Pya Y, et al. Fully Magnetically Levitated Left Ventricular Assist System for Treating Advanced HF: A Multicenter Study. J Am Coll Cardiol 2015;66:2579-89.

[53] Soucy KG, Giridharan GA, Choi Y, et al. Rotary pump speed modulation for generating pulsatile flow and phasic left ventricular volume unloading in a bovine model of chronic ischemic heart failure. J Heart Lung Transplant 2015;34:122-31.

[54] Pirbodaghi T, Weber A, Axiak S, Carrel T, Vandenberghe S. Asymmetric speed modulation of a rotary blood pump affects ventricular unloading. Eur J Cardiothorac Surg 2013;43:383-8.

[55] Amacher R, Ochsner G, Schmid Daners M. Synchronized pulsatile speed control of turbodynamic left ventricular assist devices: review and prospects. Artif Organs 2014;38:867-75.

[56] Ising MS, Sobieski MA, Slaughter MS, Koenig SC, Giridharan GA. Feasibility of Pump Speed Modulation for Restoring Vascular Pulsatility with Rotary Blood Pumps. ASAIO J 2015;61:526-32.

[57] Fihn SD, Blankenship JC, Alexander KP, et al. 2014 ACC/AHA/AATS/PCNA/SCAI/STS focused update of the guideline for the diagnosis and management of patients with stable ischemic heart disease: a report of the American College of Cardiology/American Heart Association Task Force on Practice Guidelines, and the American Association for Thoracic Surgery, Preventive Cardiovascular Nurses Association, Society for Cardiovascular Angiography and Interventions, and Society of Thoracic Surgeons. Circulation 2014;130:1749-67.

Figure legends

Figure 1. A, left. Cardiac response curves to right atrial pressure (Starling curves) in three different conditions: normal, sympathetic stimulation and damaged myocardium. A, right. Guyton's experience, from Guyton, 1955 [3]: evolution of both right atrial pressure and mean circulatory filling pressure (MCFP) as a function of blood volume, which modifies the level of MCFP, for different outputs imposed by the pump connected between the vena cava system and the aortic circuitry in freshly sacrificed dogs. As atrial pressure becomes negative compared with atmospheric pressure, the level of the venous return remains constant whatever the speed of rotation of the pump, because the suction effect of the pump limits the output of the venous return to a maximal level, attained for each circulating blood volume. B. By superposing the two graphs, Guyton could determine the cardiac output according to the right atrial pressure as the intersection point between each pair of curves. C. Illustration of simultaneous recordings at the aortic root of pressure wave, aortic flow and backward pressure reflection wave (R). In younger people, the R wave occurs during the diastolic period, whereas in the elderly, the R wave occurs before the closure of the aortic valve at the dicrotic notch (Pi), leading to an increase in both systolic (PAoS) and pulse (PAoP) aortic pressures, and to increased left ventricular stroke work. D. Sunagawa's model, modified from Morimont et al., 2009 [6]. D, left: PV loops recorded during preload reduction obtained by inflation of a balloon in the inferior vena cava, with representation of both end-systolic left ventricular (LV) elastance (Ees) and end-systolic aortic elastance (Ea) curves. D, right: PV loop with external left ventricular stroke work (SW) and amplitude of the stroke volume (arrow) determined by the intersection of the Ees and Ea curves. ESPVR: end-systolic pressure-volume relationship; PAo: aortic pressure; PAoD: diastolic aortic pressure; PVA: pressure-volume area; QAo: aortic flow.

Figure 2. A. Axial Archimedes' screw. B. Centrifugal electromagnetic spinning pump.

Figure 3. Modified from Rosenbaum et al., 2019 [19]. Synchronous high-fidelity pressure curves simultaneously monitoring aortic root (Ao) pressure (red), left ventricular (LV) pressure (grey), pulmonary artery (PA) pressure (green) and right atrial (RA) pressure (blue) on the left panel, and Ao pressure (red), LV pressure (grey), pulmonary wedge pressure (PCW; green) and RA pressure (blue)

on the right panel, at three different rotation speeds of the pumping left ventricular assistance device (from top to bottom: 9.000, 9,600 and 10,000 RPM). See text for details. EG: effective gradient; TAG: transaortic gradient.

Figure 4. Physiopathology of acquired von Willebrand syndrome, from Vincent et al., 2018 [34]. Proteolytic cleavage of von Willebrand factor (VWF) induced by high shear stress is not compensated by new VWF release (left) in a low-pulsatility system, whereas it is still compensated in a normal-pulsatility system (right). ADAMTS13: A disintegrin and metalloprotease with thrombospondin type I repeats-13; HMW: high molecular weight.

Central illustration. Physiological pulsatility along the vascular tree, with systolic (upper line), diastolic (lower line) and mean (middle line) pressures. Note the enlargement of pulse pressure in distal arteries, and the peripheral decrease in mean arterial pressure induced by arteriolar resistances. Left ventricular assistance device-induced complications, mainly because of lack of pulsatility, are shown at each level concerned. VWF: von Willebrand factor; NOS: nitric oxide synthase.

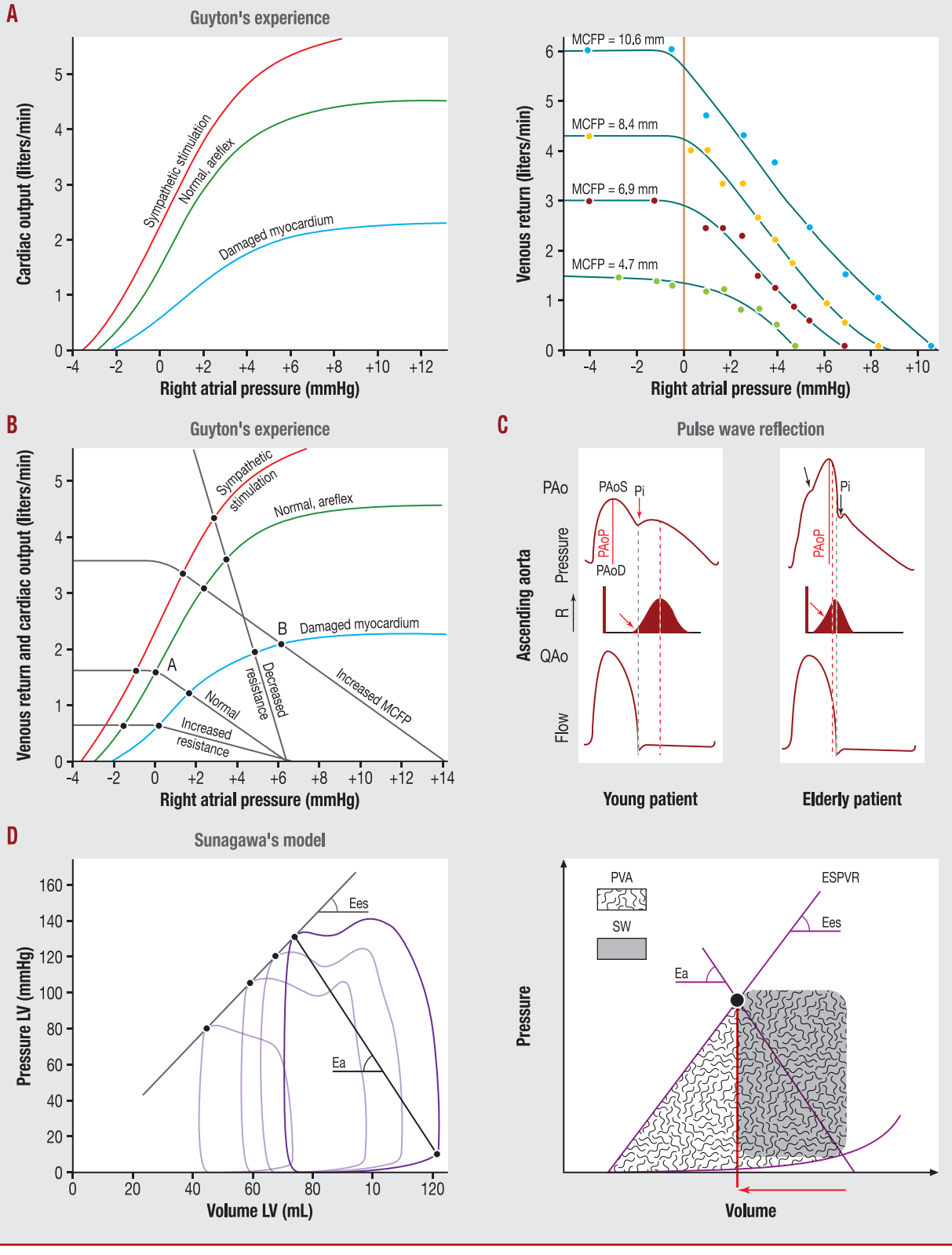
A
Guyton's experience
Cardiac output (liters/min)
Sympathetic stimulation
Normal, areflex
Damaged myocardium
Right atrial pressure (mmHg)
MCFP = 10.6 mm
MCFP = 8.4 mm
MCFP = 6.9 mm
MCFP = 4.7 mm
Venous return (liters/min)
Right atrial pressure (mmHg)
B
Guyton's experience
Venous return and cardiac output (liters/min)
Sympathetic stimulation
Normal, areflex
Damaged myocardium
A
B
Normal
Increased resistance
Decreased resistance
Increased MCFP
Right atrial pressure (mmHg)
C
Pulse wave reflection
Ascending aorta
PAo
PAoS
Pi
PAoP
PAoD
Pressure
R
QAo
Flow
Young patient
Elderly patient
D
Sunagawa's model
Pressure LV (mmHg)
Ees
Ea
Volume LV (mL)
PVA
SW
ESPVR
Ees
Ea
Pressure
Volume


A

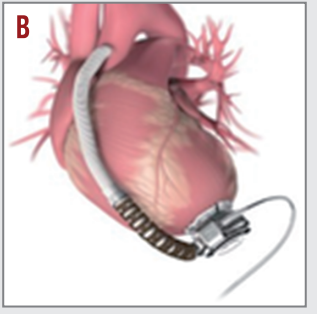
B

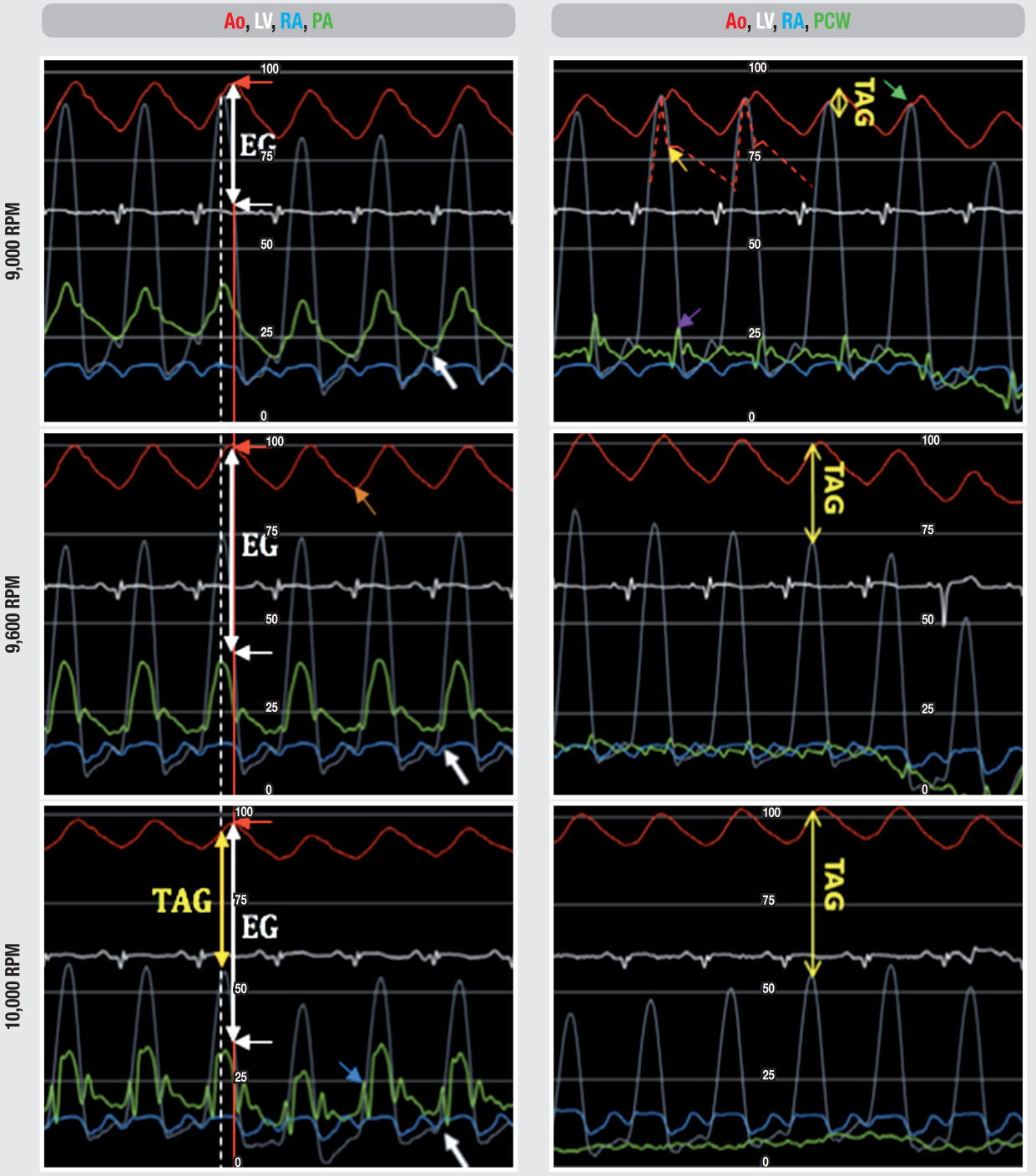
Ao, LV, RA, PA
Ao, LV, RA, PCW
9,000 RPM
9,600 RPM
10,000 RPM
EG
TAG
100
75
50
25
0

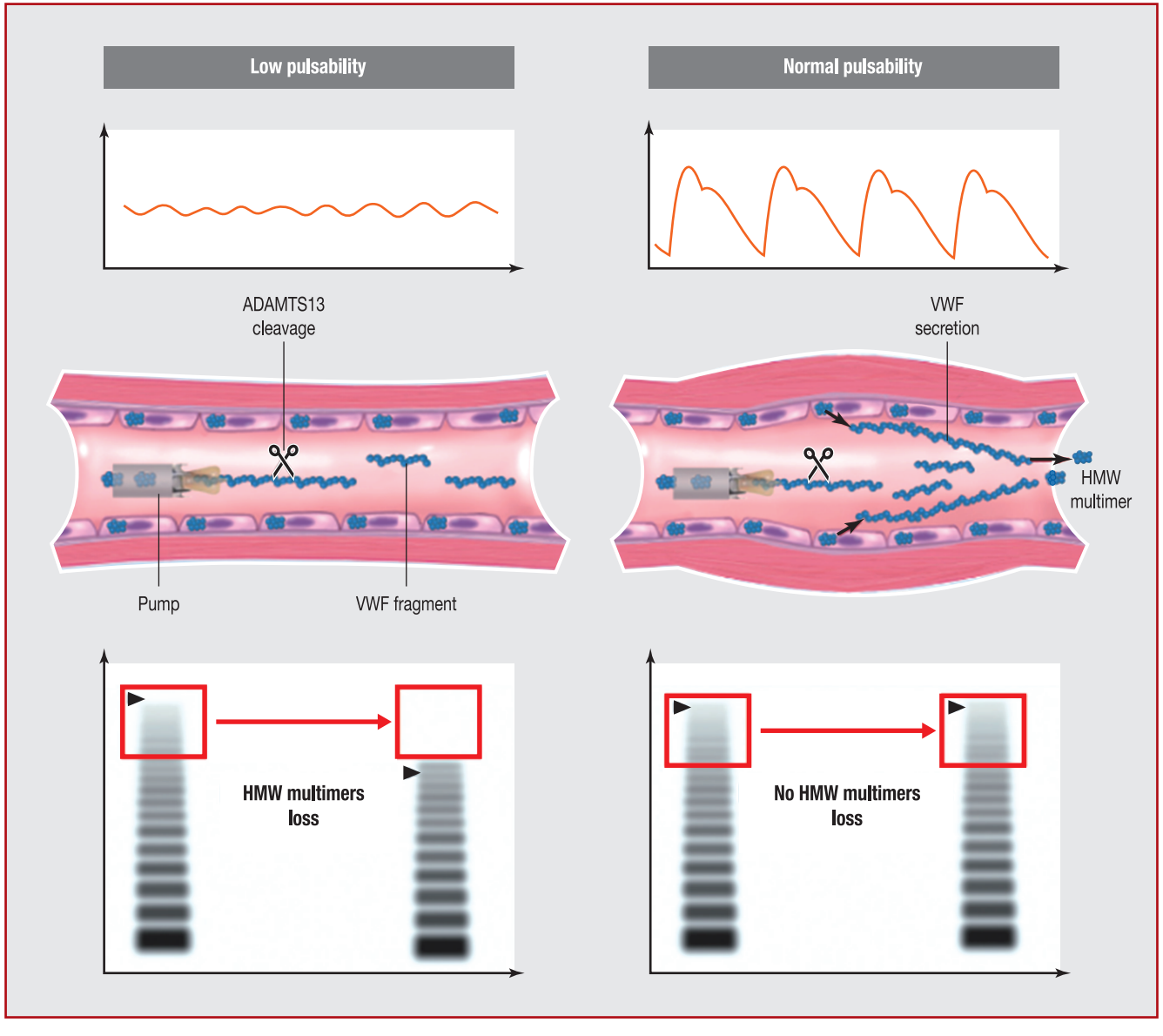
Low pulsability
Normal pulsability
ADAMTS13
cleavage
VWF
secretion
HMW
multimer
Pump
VWF fragment
HMW multimers
loss
No HMW multimers
loss

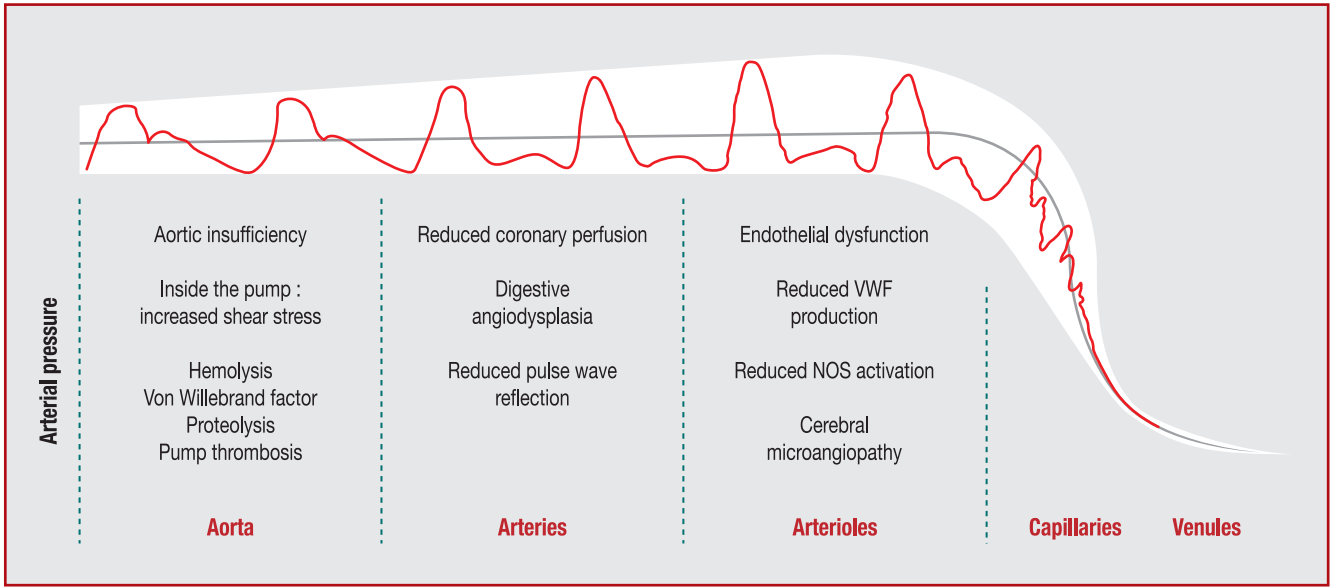
Arterial pressure
Aortic insufficiency
Inside the pump :
increased shear stress
Hemolysis
Von Willebrand factor
Proteolysis
Pump thrombosis
Aorta
Reduced coronary perfusion
Digestive
angiodysplasia
Reduced pulse wave
reflection
Arteries
Endothelial dysfunction
Reduced VWF
production
Reduced NOS activation
Cerebral
microangiopathy
Arterioles
Capillaries
Venules